

A Dual-Responsive Bola-Type Supra-amphiphile Constructed from a Water-Soluble Calix[4]pyrrole and a Tetraphenylethene-Containing Pyridine Bis-*N*-oxide

Xiaodong Chi, Huacheng Zhang, Gabriela I. Vargas-Zúñiga, Gretchen M. Peters, and Jonathan L. Sessler*

Department of Chemistry, The University of Texas at Austin, 105 East 24th Street, Stop A5300, Austin, Texas 78712-1224, United States

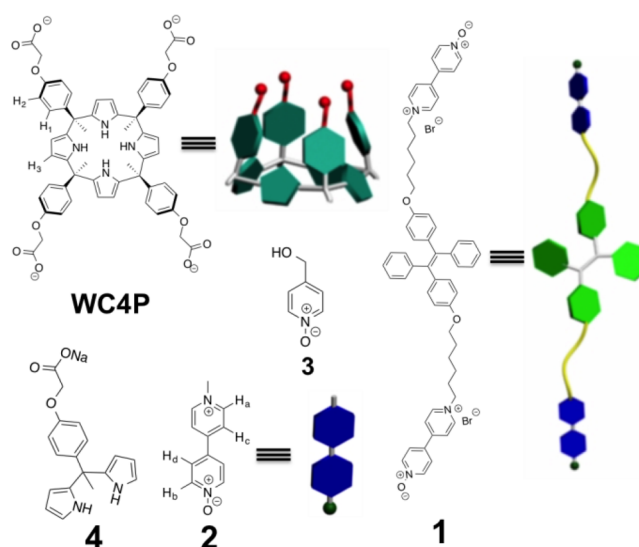
S Supporting Information

ABSTRACT: Complexation between a water-soluble calix[4]pyrrole and a ditopic pyridine *N*-oxide derivative in aqueous media produces a bola-type supra-amphiphile that self-assembles to produce higher order morphologies, including multilamellar vesicles and micelles depending on the pH. The present bola-type supra-amphiphile exhibits strong fluorescence due to structural changes and aggregation induced by host–guest complexation. The resulting structures may be used to recognize, encapsulate, and release non-fluorescent, water-soluble small molecules.

Macrocyclic receptors that can be used to assemble supra-amphiphiles through guest encapsulation in aqueous milieus are of interest because they can be used to create a wide variety of higher order morphologies, including vesicles, micelles, nanotubes, and nanoribbons.¹ The resulting self-assembled constructs are attractive for use in a wide variety of fields, such as drug/gene delivery, cell imaging, and fuel storage.² To date, a variety of receptor systems, including crown ethers, cucubiturils, cyclodextrins, calixarenes, and pillarenes, have been used to create supra-amphiphiles.^{3–7} Calix[4]pyrroles are another well-recognized class of receptors. Calix[4]pyrroles are macrocycles consisting of four pyrrole units linked by fully substituted sp³ hybridized *meso*-carbon atoms.⁸ To date, calix[4]pyrroles have been used to create supramolecular polymers,⁹ ion-pair receptors,¹⁰ anion transport agents,¹¹ and sensors,¹² albeit in noncompetitive solvent environments.¹³ Recently, Ballester et al. reported a water-soluble, aryl-extended calix[4]pyrrole system. In this case, complexation of pyridine *N*-oxide derivatives was achieved under aqueous conditions via a combination of hydrophobic and hydrogen bond interactions that stabilize guest binding deep within the aromatic cavity of the calix[4]pyrrole receptor. The result was formation of a capsule.^{8d,14} Here we report the use of water-solubilized calix[4]pyrroles in conjunction with appropriately designed ditopic pyridine *N*-oxide guests to create bola-type amphiphiles.

The present bola-type amphiphile relies on the recognition of a tetraphenylethene (TPE) pyridine *N*-oxide derivative (1) by a water-soluble aryl extended calix[4]pyrrole (WC4P) (Scheme 1). This complexation occurs in water and is pH dependent. Under neutral or basic conditions, the interaction between 1 and WC4P produces a supra-amphiphile, which undergoes further self-assembly to form vesicles. The pH-responsive

Scheme 1. Structures of WC4P, 1, Model Guests 2, 3, and Model Host 4



nature of the host–guest interaction between WC4P and guest 1 allows for the reversible interconversion between the self-assembled vesicles and small solid nanoparticles as a function of pH.

Prior to studying the proposed self-assembly processes, ¹H NMR spectroscopic studies were carried out to characterize the pyridine *N*-oxide binding properties of WC4P. Due to the relatively poor water-solubility of 1, the monofunctional pyridine *N*-oxide 2 was used for these experiments. As shown in Figure 1, when 1.0 equiv of 2 was added to a solution of WC4P in D₂O, substantial shifts in the signals for both the host and the guest were observed. These changes were consistent with the *N*-oxide functionality in 2 lying deep within the cavity formed by WC4P.

To characterize the supramolecular complex WC4P⊃2 in greater detail, 2D nuclear Overhauser effect spectroscopy (NOESY) experiments were carried out (Figure S11). Strong nuclear Overhauser effect (NOE) correlations were observed between the signals corresponding to protons H_b and H_d on guest 2 and protons H₁ and H₂ of WC4P (For peak

Received: March 26, 2016

Published: April 28, 2016

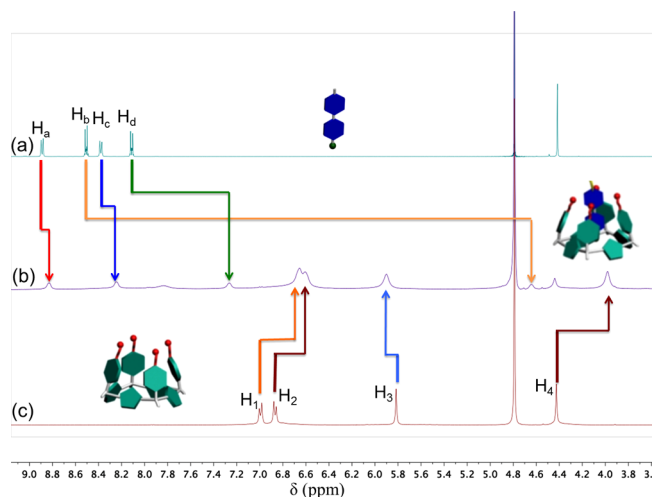


Figure 1. Partial ^1H NMR spectra (400 MHz, D_2O , 25 $^\circ\text{C}$) of (a) **2** alone (2.00 mM); (b) 2.00 mM **2** and 2.00 mM **WC4P**; and (c) **WC4P** alone (2.00 mM).

assignments see Figure S11). These observations provide further support for the conclusion that **2** is indeed deeply embedded within the cavity defined by **WC4P**.

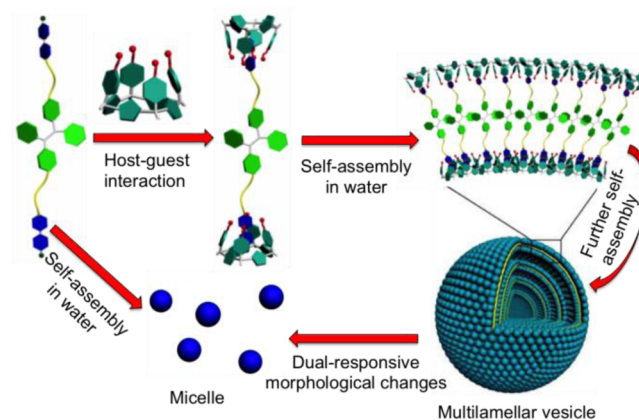
A mole ratio plot based on a UV–vis spectroscopic titration revealed a maximum consistent with the formation of a 1:1 inclusion complex between **WC4P** and **2** in water (Figure S14c). Using nonlinear curve-fitting methods, an association constant, $K_a = (1.43 \pm 0.12) \times 10^4 \text{ M}^{-1}$, corresponding to the formation of **WC4P**⊃**2** could be calculated from these titrations (Figure S14b). The formation of this complex was further confirmed by electrospray ionization mass spectrometry (ESI-MS); cf. Figure S10.

It is well-established that neutral carboxylic acid groups and anionic carboxylate groups can be interconverted reversibly by adjusting the solution pH.¹⁵ Therefore, the pH-dependent behavior of **WC4P**⊃**2** complex was studied by first lowering the solution pH (initially at pH 7.4) to 4.0 by adding HCl. This led to precipitation of the protonated (carboxylic acid) form of **WC4P** and release of guest **2**. Support for the proton-induced decomplexation came from ^1H NMR spectroscopic analyses, which revealed the disappearance of the signals corresponding to H_1 , H_2 , and H_3 of the **WC4P** host. Moreover, only signals corresponding to free **2** were seen in the deuterated supernatant (Figure S19b). When the pH was adjusted back to 7.4 by adding sodium hydroxide, the precipitate dissolved. Presumably, this reflects reformation of **WC4P**⊃**2**, a conclusion supported by ^1H NMR spectral studies (cf. Figure S19c).

The release engendered by the addition of HCl to **WC4P**⊃**2** is ascribed to protonation rather than competition from the chloride anion. As shown in Figure S12, when 3.0 equiv of TBACl was added to a mixture of **WC4P** and **2** at pH 7.4, the proton chemical shift of **2** underwent little change. On the other hand, when 2.0 equiv of **3** was added to a D_2O solution of **2** and **WC4P** (both 2.0 mM), the signals corresponding to **3** underwent an upfield shift while those for **2** shifted back to those of the free form (cf. Figure S13). Such findings are consistent with **3** acting as a competitive guest and displacing **2**.

The above studies led us to consider that a ditopic pyridine *N*-oxide could be used to promote the formation of supramolecular aggregates. To test this hypothesis, we prepared the functionalized amphiphile **1** (Scheme 2). Initial support for the formation of a supramolecular complex between **1** and

Scheme 2. Schematic Illustration of the Self-Assembly Processes That Lead to the Formation of Calix[4]pyrrole-Based Bola-Type Supra-amphiphiles and Their Self-Assembly into Multimellar Stacked Vesicles; Also Shown Is Their pH-Triggered Vesicle-to-Micelle Transition



WC4P came from fluorescence spectroscopy. As shown in Figure 2a, the amphiphile **1** ($5.00 \times 10^{-5} \text{ M}$) alone showed almost no fluorescence in water (Figure 2a, red line). This lack of appreciable emission intensity for the free form of **1** is

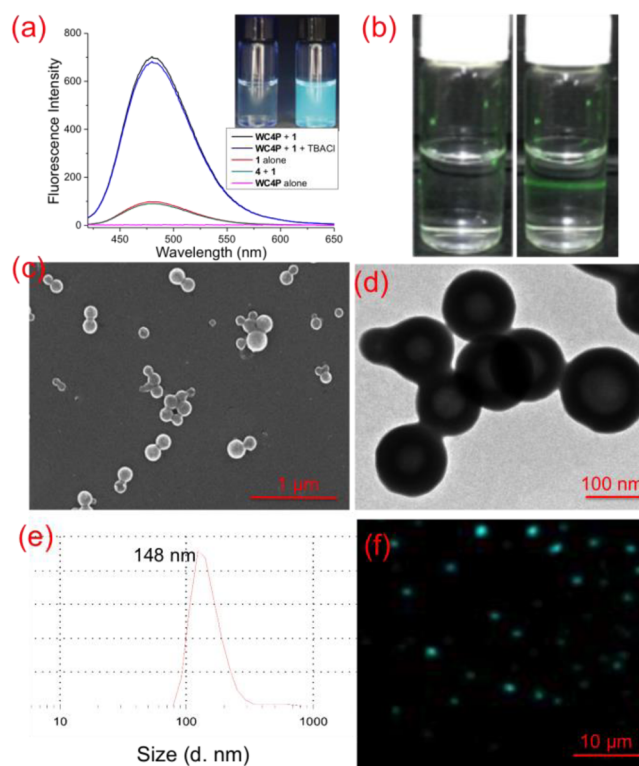


Figure 2. (a) Fluorescence spectra of **1** (red line), **4 + 1** (cyan line), a 1:2 mixture of **1** ($5.00 \times 10^{-5} \text{ M}$) and **WC4P** (black line), and the latter solution + TBACl (blue line)¹⁷ $\lambda_{\text{ex}} = 340 \text{ nm}$ in H_2O , inset: Photographs of **1** (left) and **1 + WC4P** (right) excited using a 365 nm UV light source. (b) Tyndall effect (left: **1** alone; right: **WC4P + 1**). (c) SEM image of aggregates formed from a mixture of **WC4P** and **1** at 25 $^\circ\text{C}$. (d) TEM image of **WC4P + 1** aggregates at 25 $^\circ\text{C}$. (e) DLS data for aggregates formed from a mixture of **WC4P** and **1** at 25 $^\circ\text{C}$. (f) Fluorescence microscopic image of the aggregates. ($[\text{WC4P}] = 3.0 \times 10^{-4} \text{ M}$, $[\mathbf{1}] = 1.5 \times 10^{-4} \text{ M}$).

ascribed to interactions between the constituent TPE subunits, which are favored in the polar aqueous medium. However, when 2.0 equiv of WC4P was added to this solution, the fluorescence intensity increased dramatically (Figure 2a, black line). Presumably, this increase is due to the fact that the rotation of the phenyl rings of **1** becomes restricted upon the addition of WC4P. Therefore, the fluorescence intensity increases,¹⁶ a finding that is consistent with the results of Liu and co-workers.^{16b} In a control experiment, compound **4** (corresponding to a substructure of WC4P) was added in excess to an aqueous solution of **1**. No appreciable change in the fluorescence of **1** was seen (Figure 2a, green line).

By monitoring the concentration-dependent surface tension, the critical aggregation concentration (CAC) of **1** was calculated to be ca. 1.2×10^{-4} M (Figure S13). The CAC of **1** recorded in the presence of WC4P was lower by more than a factor of 20 (CAC of WC4P>**1** = 5.3×10^{-6} M) (Figure S14). This decrease in the CAC of **1** in the presence of WC4P is ascribed to the formation of a stable host-guest complex with WC4P. Furthermore, a solution of WC4P (1.00×10^{-4} M) and **1** (5.00×10^{-5} M) in water shows a Tyndall effect, something that is not observed for a 5.00×10^{-5} M aqueous solutions of **1** alone (Figure 2b). Such findings are consistent with self-assembled aggregates being formed from 1:2 mixtures of **1** and WC4P, not for the individual components.

Scanning electron microscopy (SEM) and transmission electron microscopy (TEM) were used to study the presumed self-assembled aggregates (Figure 2c,d). Both studies were consistent with the formation of spherical aggregates with an average diameter of about 160 nm (Figure 2c). From the TEM studies, the thickness of the vesicle walls was calculated to be about 30 nm (Figure 2d). Dynamic light scattering (DLS) analyses revealed that the average size of these self-assembled ensembles was ~148 nm (Figure 2e), Confocal fluorescence images showed that the aggregates formed from WC4P>**1** under these conditions exhibited strong blue fluorescence (Figure 2f).

The morphological changes of the aggregates formed from WC4P + **1** were analyzed at two different pH values using TEM. As shown in Figure 3a, solid nanoparticles with a

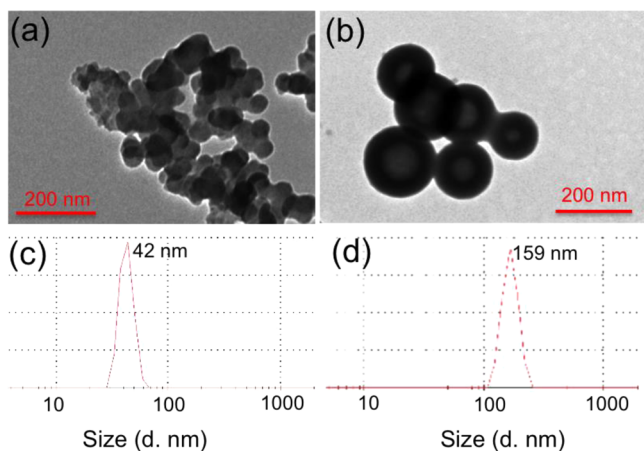


Figure 3. TEM images of (a) the aggregates formed from WC4P + **1** when the pH of the solution is 4.0 and 7.4 (b). Results of DLS studies involving (c) the aggregates formed from WC4P + **1** when the pH of the solution is 4.0 and 7.4 (d). ([WC4P] = 3.0×10^{-4} M, [**1**] = 1.5×10^{-4} M).

diameter of about 40 nm appeared when the pH of the solution was adjusted to pH 4.0 by adding HCl. However, when the pH was adjusted back to 7.4 via the addition of NaOH_{aq}, vesicles analogous to those obtained originally at near-neutral pH were again observed (Figure 3b). DLS measurements revealed concordant size differences as a function of pH (Figure 3c,d). The chemical responsive behavior seen for WC4P>**2** when exposed to competitor **3** were reproduced in the case of the aggregates formed from WC4P>**1** (cf. Figure S18).

A graphic model of the supramolecular recognition and self-assembly processes that occur when 2 equiv of WC4P is mixed with **1** is shown in Scheme 2. Briefly, we suggest that upon complexation, the two pyridine *N*-oxide subunits of **1** bind to WC4P resulting in the formation a bola-type supra-amphiphile, which then further self-assembles to form a bilayer structure that curves back on itself to generate multilamellar spheres. Acidic conditions induce the precipitation of WC4P from water, which releases **1** in the form of small solid nanoparticles. Release can also be engendered via the addition of a competitive guest (**3**) that contains a pyridine *N*-oxide subunit.

To date, stimuli-responsive self-assembled materials have been used to capture and release various cargoes, including inherently fluorescent encapsulated drugs.¹⁸ However, the release of non-fluorescent drugs cannot easily be monitored by these means. Our system involves fluorescent components whose emission intensity increases as the aggregates it forms are destroyed by lowering the pH or via the addition of a competitive guest (i.e., **3**).

To test whether our system could be used with non-fluorescent payloads, we chose gemcitabine (a widely used anti-cancer chemotherapeutic agent) as a model non-fluorescent drug. As the pH of the solution containing gemcitabine and WC4P>**1** was decreased from 7.4 to 4.0, the fluorescence intensity of the vesicles decreased (Figure 4a, cyan blue line).

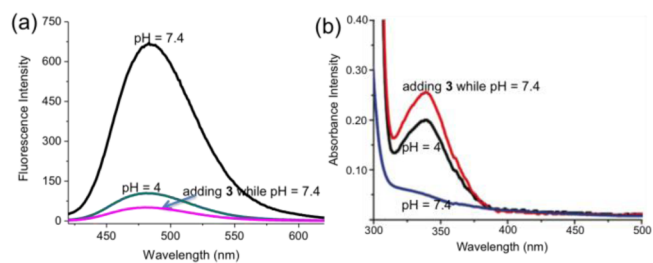


Figure 4. (a) Fluorescence emission spectra (WC4P>**1** with gemcitabine inside the vesicle), $\lambda_{\text{ex}} = 340$ nm; (b) UV-vis spectra of the supramolecular vesicle solution (with gemcitabine inside) upon the addition of acid. The concentration of the WC4P>**1** is 8.0×10^{-5} M.

Concurrently, the absorbance intensity of the gemcitabine increased (Figure 4b, black line). A similar fluorescence intensity decrease was seen upon adding the competitive guest **3**. These changes are consistent with the gemcitabine, initially encapsulated in the vesicles, being released into the aqueous medium.¹⁹

In summary, we have successfully created a water-soluble pH-responsive calix[4]pyrrole-based molecular recognition motif, WC4P. In the presence of the ditopic pyridine bis-*N*-oxide **1**, WC4P forms a bola-type supra-amphiphile (WC4P>**1**), which self-assembles to form fluorescent vesicles in water. This system is responsive both to pH and chemical competitors (e.g., **3**). Breakup of the supramolecular vesicles

generated from WC4P>1 releases **1** in the form of small nanoparticles and represents a responsive switch effect that has been successfully applied to the controlled release of gemcitabine. An advantage of the present system is that it allows the uptake and release of non-fluorescence payload to be followed by optical means. The present work also serves to show that calix[4]pyrroles can be used to create self-assembled materials in aqueous environments.

■ ASSOCIATED CONTENT

📄 Supporting Information

The Supporting Information is available free of charge on the ACS Publications website at DOI: [10.1021/jacs.6b03159](https://doi.org/10.1021/jacs.6b03159).

Experimental details and characterization data (PDF)

■ AUTHOR INFORMATION

Corresponding Author

*sessler@cm.utexas.edu

Notes

The authors declare no competing financial interest.

■ ACKNOWLEDGMENTS

The work was supported by the U.S. National Science Foundation (grant CHE-1402004) and the R. A. Welch Foundation (Grant F-1018).

■ REFERENCES

- (1) (a) Harada, A.; Hashidzume, A.; Yamaguchi, H.; Takashima, Y. *Chem. Rev.* **2009**, *109*, 5974. (b) Xue, M.; Yang, Y.; Chi, X.; Zhang, Z.; Huang, F. *Acc. Chem. Res.* **2012**, *45*, 1294. (c) Appel, E. A.; Loh, X. J.; Jones, S. T.; Biedermann, F.; Dreiss, C. A.; Scherman, O. A. *J. Am. Chem. Soc.* **2012**, *134*, 11767. (d) Wang, M.-X. *Acc. Chem. Res.* **2012**, *45*, 182. (e) Wang, C.; Wang, Z.; Zhang, X. *Acc. Chem. Res.* **2012**, *45*, 608. (f) Guo, D.-S.; Liu, Y. *Acc. Chem. Res.* **2014**, *47*, 1925. (g) Qi, Z.; Schalley, C. A. *Acc. Chem. Res.* **2014**, *47*, 2222. (h) Ma, X.; Tian, H. *Acc. Chem. Res.* **2014**, *47*, 1971. (i) Li, C. *Chem. Commun.* **2014**, *50*, 12420. (j) Jie, K.; Zhou, Y.; Yao, Y.; Huang, F. *Chem. Soc. Rev.* **2015**, *44*, 3568. (k) Jordan, J. H.; Gibb, B. C. *Chem. Soc. Rev.* **2015**, *44*, 547.
- (2) (a) Ravoo, B. J.; Jacquier, J.-C.; Wenz, G. *Angew. Chem., Int. Ed.* **2003**, *42*, 2066. (b) Li, Y.; Park, T.; Quansah, J. K.; Zimmerman, S. C. *J. Am. Chem. Soc.* **2011**, *133*, 17118. (c) Kumar, R.; Lee, Y. O.; Bhalla, V.; Kumar, M.; Kim, J. S. *Chem. Soc. Rev.* **2014**, *43*, 4824. (d) Chi, X.; Ji, X.; Xia, D.; Huang, F. *J. Am. Chem. Soc.* **2015**, *137*, 1440. (e) Ma, X.; Zhao, Y. *Chem. Rev.* **2015**, *115*, 7794.
- (3) (a) Chen, L.; Tian, Y.; Ding, Y.; Tian, Y.; Wang, F. *Macromolecules* **2012**, *45*, 8412. (b) Ji, X.; Dong, S.; Wei, P.; Xia, D.; Huang, F. *Adv. Mater.* **2013**, *25*, 5725.
- (4) Nalluri, S. K. M.; Voskuhl, J.; Bultema, J. B.; Boekema, E. J.; Ravoo, B. J. *Angew. Chem., Int. Ed.* **2011**, *50*, 9747.
- (5) Lee, M. L.; Lee, S.-J.; Jiang, L.-H. *J. Am. Chem. Soc.* **2004**, *126*, 12724.
- (6) Lee, H.-K.; Park, K. M.; Jeon, Y. J.; Kim, D.; Oh, D. H.; Kim, H. S.; Park, C. K.; Kim, K. *J. Am. Chem. Soc.* **2005**, *127*, 5006.
- (7) Cao, Y.; Hu, X.-Y.; Li, Y.; Zou, X.; Xiong, S.; Lin, C.; Shen, Y.-Z.; Wang, L. *J. Am. Chem. Soc.* **2014**, *136*, 10762.
- (8) (a) Gale, P. A.; Sessler, J. L.; Král, V.; Lynch, V. *J. Am. Chem. Soc.* **1996**, *118*, 5140. (b) Gale, P. A.; Sessler, J. L.; Král, V. *Chem. Commun.* **1998**, *1*. (c) Gil-Ramírez, G.; Escudero-Adán, E. C.; Benet-Buchholz, J.; Ballester, P. *Angew. Chem., Int. Ed.* **2008**, *47*, 4114. (d) Verdejo, B.; Gil-Ramírez, G.; Ballester, P. *J. Am. Chem. Soc.* **2009**, *131*, 3178. (e) Slovak, S.; Evan-Salem, T.; Cohen, Y. *Org. Lett.* **2010**, *12*, 4864.
- (9) (a) Verdejo, B.; Rodríguez-Llansola, F.; Escuder, B.; Miravet, J. F.; Ballester, P. *Chem. Commun.* **2011**, *47*, 2017. (b) Kim, D. S.; Chang, J.; Leem, S.; Park, J. S.; Thordarson, P.; Sessler, J. L. *J. Am. Chem. Soc.* **2015**, *137*, 16038.

(10) (a) Ciardi, M.; Galán, A.; Ballester, P. *J. Am. Chem. Soc.* **2015**, *137*, 2047. (b) Kim, S. K.; Sessler, J. L. *Acc. Chem. Res.* **2014**, *47*, 2525.

(11) (a) Adriaenssens, L.; Estarellas, C.; Jentzsch, A. V.; Belmonte, M. M.; Matile, S.; Ballester, P. *J. Am. Chem. Soc.* **2013**, *135*, 8324. (b) Kim, D. S.; Sessler, J. L. *Chem. Soc. Rev.* **2015**, *44*, 532.

(12) (a) Anzenbacher, P.; Jursíková, K., Jr.; Sessler, J. L. *J. Am. Chem. Soc.* **2000**, *122*, 9350. (b) Liu, Y.; Minami, T.; Nishiyabu, R.; Wang, Z.; Anzenbacher, P., Jr. *J. Am. Chem. Soc.* **2013**, *135*, 7705.

(13) (a) Allen, W. E.; Gale, P. A.; Brown, C. T.; Lynch, V. M.; Sessler, J. L. *J. Am. Chem. Soc.* **1996**, *118*, 12471. (b) Gale, P. A.; Sessler, J. L.; Kral, V.; Lynch, V. *J. Am. Chem. Soc.* **1996**, *118*, 5140.

(14) Hernández-Alonso, D.; Zankowski, S.; Adriaenssens, L.; Ballester, P. *Org. Biomol. Chem.* **2015**, *13*, 1022.

(15) Duan, Q.; Cao, Y.; Li, Y.; Hu, X.; Xiao, T.; Lin, C.; Pan, Y.; Wang, L. *J. Am. Chem. Soc.* **2013**, *135*, 10542.

(16) (a) Hong, Y.; Lam, J. W. Y.; Tang, B. Z. *Chem. Commun.* **2009**, 4332. (b) Jiang, B.-P.; Guo, D.-S.; Liu, Y.-C.; Wang, K.-P.; Liu, Y. *ACS Nano* **2014**, *8*, 1609. (c) Wang, P.; Yan, X.; Huang, F. *Chem. Commun.* **2014**, *50*, 5017.

(17) Almost no change in the fluorescence signature was seen when TBACl was added to the host–guest complex WC4P>2.

(18) Reinhout, I. C.; Cornelissen, J. J. L. M.; Nolte, R. J. M. *Acc. Chem. Res.* **2009**, *42*, 681.

(19) Zhu, S.; Lansakara-P, D. S. P.; Li, X.; Cui, Z. *Bioconjugate Chem.* **2012**, *23*, 966.